ChemComm

COMMUNICATION

View Article Online
View Journal

Cite this: DOI: 10.1039/d0cc05788f

Received 26th August 2020,
Accepted 1st October 2020

DOI: 10.1039/d0cc05788f

rsc.li/chemcomm

Combining API in a dual-drug ternary cocrystal approach†

Lixing Song, [a] Koen Robeyns, [a] Nikolay Tumanov, [b] Johan Wouters [b] and Tom Leyssens *[a]

A new strategy is developed to design multi-drug solid forms. Using an inorganic salt as the glue sticking together two different APIs in a "drug-bridge-drug" approach, we successfully created and characterized three different ternary ionic cocrystals (TICCs). The link between binary and ternary ICCs and the importance of reaction stoichiometry was investigated using ternary solid-state phase diagrams. In addition, we highlighted the crucial role of water for the stability of these systems, as well as the impact on solubility compared to the respective parent compounds. We expect the strategy presented here to be applicable to a large series of drug combinations, opening up a promising new way of building multi-drug systems.

The combination of multiple drugs is a popular way to obtain a synergistic or stronger therapeutic effect. Fixed-dose combination (FDC) is a traditional method to combine two or more drugs into a single dosage form.[1] However, the advantages of FDC are restricted because of issues regarding stability, differences of solubility and incompatibility between different drugs.[2] Multi-drug cocrystallization[3,4] is an alternative method to overcome these issues as cocrystals have the potential to modulate physicochemical properties. A formulation of cocrystals of sacubitril and disodium valsartan,[5] the first multi-drug cocrystal approved by the FDA in 2015, is used for the treatment of heart failure with reduced ejection fraction relative to separated drugs.

However, successful cocrystallization of two compounds is not straightforward as the intermolecular interactions in the novel crystal form need to be more stable than the ones in the separate parent solid forms. This implies that one cannot freely choose the two components to cocrystallize, rendering the multi-drug cocrystal approach rather serendipitous. To deal with this problem, Liu *et al.* introduced[6] a "drug-bridge-drug" strategy, linking the antitubercular drugs isoniazid and pyrazinamide using fumaric acid as a bridge in a molecular cocrystal. Although very interesting, this strategy remains challenging, partly due to the difficulty in identifying an appropriate bridge. The ternary cocrystal needs to be more stable than the solid form of any of the binary combinations and/or parent compounds,[7] and moreover, is required to be pharmaceutically acceptable. As organic molecular cocrystals are often only stabilized by a few kcal mol^{-1} with respect to their parent compounds, this approach seems limited. Over the last years, however, ionic cocrystals (ICCs) have been introduced as alternatives to molecular cocrystals.[7–13] ICCs consist of an organic compound cocrystallized with an inorganic salt, which can be advantageous compared with molecular cocrystals due to the fact that stronger interactions occur between the metal and the target compound.[14] Ionic cocrystallization is a promising field of research, as the salts used are often pharmaceutically accepted, and easily lead to cocrystallization with drug compounds.[15–22] In the ICC the central metal atom often links to multiple organic molecules. Considering the higher stability of the ionic cocrystals, the fact that metal atom can easily accommodate different ligands, and that inorganic salts are often biologically accepted, these salts could potentially serve as the perfect linker to ternary cocrystal systems comprising two different APIs. Up to now there has only been a single ternary ionic cocrystal (TICC) $[Zn(thiourea)(urea)Cl_2]$ reported showing increased fertilization efficiency.[23] In this paper, we tap into this unexplored barrel, using inorganic salts as a bridge to cocrystallize two parent drug compounds, which without this linker do not cocrystallize.

Levetiracetam ((*S*)-2-(2-oxopyrrolidin-1-yl)butanamide, LEV) is a commonly used anti-epileptic drug developed by UCB Pharma[24] and etiracetam (ETI) is its racemic intermediate[25] (Fig. 1). Nicotinamide (pyridine-3-carboxamide, NA) is a vitamin from the vitamin B group and used as dietary supplement and medication.[26] Isonicotinamide (pyridine-4-carboxamide, INA)

[a] *Institute of Condensed Matter and Nanosciences, Université catholique de Louvain, 1 Place Louis Pasteur, B-1348 Louvain-La-Neuve, Belgium. E-mail: tom.leyssens@uclouvain.be*

[b] *Unité de Chimie Physique Théorique et Structurale, Chemistry Department, Namur Institute of Structured Matter (NISM), University of Namur, 61 rue de Bruxelles, B-5000 Namur, Belgium*

† Electronic supplementary information (ESI) available: Materials and methods, screening, structural characteristics, solid-state reaction, DSC, TGA, VT-XRPD and solution behavior. CCDC 2025075–2025077. For ESI and crystallographic data in CIF or other electronic format see DOI: 10.1039/d0cc05788f

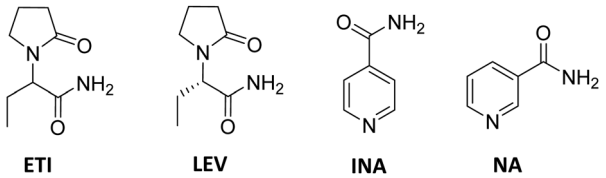

Fig. 1 Chemical structures of model compounds.

is an isomer of NA and both are popular cocrystal formers.[27–30] In previous work, we investigated the cocrystallization between $CaCl_2$ and LEV/ETI showing the successful formation of dihydrate ionic cocrystals.[31] In parallel, INA and NA were reported to form ionic cocrystals with $CaCl_2$.[15,32,33] LEV and or ETI in turn do not form a cocrystal with INA nor NA. This system is therefore ideal to demonstrate the potential of our ionic linker strategy. We successfully show how our strategy can be used to glue two drugs using a salt as binder. We furthermore highlight the thermodynamics behind this approach investigating the solid-state ternary phase diagrams of these systems. Finally, we insist on the physicochemical improvements TICCs can achieve with respect to binary ICCs, as well as to the parent compounds.

As ETI/LEV and INA/NA form binary ICCs with $CaCl_2$, we were convinced the central Ca^{2+} cation could potentially link two different ligands/drugs in a dual-drug approach. To verify, ternary cocrystal combinations were explored using a variety of methods (liquid assisted grinding, slurry crystallization and solution evaporation, which are all detailed in the ESI†). Out of the four possible drug/drug combinations, three successfully led to the formation of dual-drug TICCs as hypothesized: $ETI_2{\cdot}INA{\cdot}CaCl_2{\cdot}H_2O$ (TICC1), $LEV_2{\cdot}INA{\cdot}CaCl_2{\cdot}H_2O$ (TICC2) and $LEV_2{\cdot}NA{\cdot}CaCl_2{\cdot}H_2O$ (TICC3). All methods tried led to the same TICC solid form, no TICC was observed for the ETI–NA–$CaCl_2$ system observed during the entire screening process. Furthermore, when grinding TICC3 with ETI, TICC3 was dismantled into a mixture of $ETI_2{\cdot}CaCl_2{\cdot}H_2O$, NA and LEV, which highlights the high stability of the binary $ETI_2{\cdot}CaCl_2{\cdot}H_2O$ cocrystal, likely explaining why the ternary cocrystal is not formed. We were able to grow single crystals of TICC1, TICC2, and TICC3. For all, the simulated XRPD patterns from the single crystal data, aligned with the XRPD data of the screening experiments.

For the INA involving ternary cocrystals, TICC1 and TICC2, identical coordination around the Ca^{2+} cation is observed respectively for the racemic and enantiopure cocrystal. The Ca^{2+} cation shows an octahedral coordination connecting the oxygen atoms of 4 racetam molecules (2 molecules linking through their amide oxygen atom and two molecules linking through the oxygen atom of the pyrrolidinone group), one oxygen atom of INA and one oxygen atom of a water molecule. Each racetam molecule interacts with two Ca^{2+} ions respectively through its amide and pyrrolidinone groups and serves as a bridge between consecutive Ca^{2+} cations, leading to an overall 2 : 1 : 1 (racetam : INA : $CaCl_2$) stoichiometry (Fig. 2a) and a 1D chain along the *a* axis. The infinite chain involves hydrogen bonds between chloride ions and NH_2 groups or water molecules (Fig. 2b). The chains are held together *via* hydrogen bonds between chloride ions and amide NH_2 groups of INA molecules

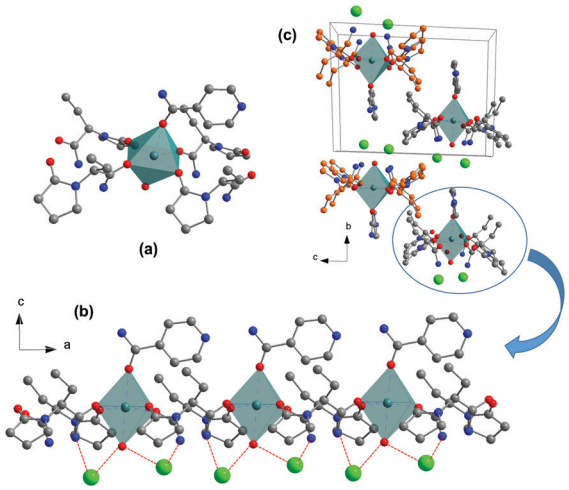

Fig. 2 (a) Coordination around the Ca^{2+} cation in crystalline TICC1 and TICC2. (b) Chain and hydrogen bonds along the *a* axis. (c) Parallel chains projected down the *a* axis in crystalline TICC1. ETI with opposite chirality are shown in grey and orange. Hydrogen atoms are omitted for clarity.

(Table S3, ESI†). In TICC1, the calcium cations coordinate four racetam molecules of the same chirality consistent with the binary ionic cocrystal $ETI_2{\cdot}CaCl_2{\cdot}2H_2O$ reported in previous work.[31] This leads to isochiral strands alternating in the racemic cocrystal (Fig. 2c). Cocrystallization of LEV, NA and $CaCl_2$ led to the formation of TICC3. In TICC3, the Ca^{2+} cation also shows an octahedral coordination connecting four LEV molecules, one water molecule and one NA molecule by the heterocyclic nitrogen instead of the carbonyl group (Fig. 3). This leads to a 1D chain structure along the *b* axis including hydrogen bonds between chloride ions and NH_2 groups or water molecules. Surprisingly, $CaCl_2$ is not able to couple the racemic counterpart ETI with NA, highlighting the small free energy difference associated with cocrystal forming systems, and hence the impact chirality can have on successful cocrystal formation.[34]

To validate the thermodynamic stability of the observed TICCs and to investigate the relation between parent compounds, binary

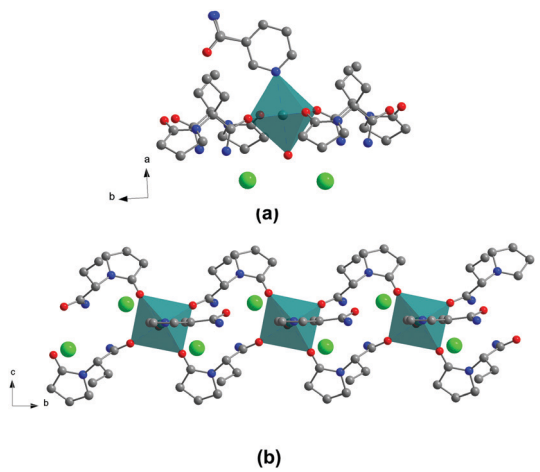

Fig. 3 (a) Coordination around the Ca^{2+} cation in TICC3. (b) Infinite chain along the *b* axis for TICC3.

and ternary systems, a full thermodynamic solid-state phase diagram was constructed, through a series of mechanochemical reactions on different ratios of LEV/ETI, INA/NA and $CaCl_2$. To assure equilibrium was reached upon grinding, experiments were performed for long reaction time, and seeded using different forms.‡ As the three TICC systems behave similarly, the LEV–INA–$CaCl_2$ system is discussed here and the results of other two systems are reported in the ESI.†

Grinding a 2 : 1 ratio of LEV : $CaCl_2$ or INA : $CaCl_2$ leads to the binary ionic cocrystals $LEV_2{\cdot}CaCl_2{\cdot}2H_2O$ (ICC1) or $INA_2{\cdot}CaCl_2{\cdot}4H_2O$ (ICC2). TICC2 can then be obtained through various routes. One can either start from the initial reactants in a 2 : 1 : 1 ratio, from ICC1 adding an equivalent of INA, or from ICC2 adding 4 equivalents of LEV and one equivalent of $CaCl_2$. Grinding ICC1 and ICC2 together leads to a physical mixture of these two forms, unless the necessary amount of LEV and $CaCl_2$ is added to this mixture to assure an overall 2 : 1 : 1 ratio. Gradually adding $CaCl_2$ to TICC2, transforms this latter into ICC1 and ICC2 with addition of sufficient $CaCl_2$ ultimately leading to a full transformation (Scheme 1 and experimental data see Fig. S4, ESI†). These experiments show that for a given overall composition, there is only one thermodynamic outcome. This scheme, as well as the phase diagram discussed below, also highlight the importance of stoichiometry when screening for dual-drug ternary cocrystals, as an initial mishap in stoichiometry may lead to a false negative *e.g.* an excessive amount of $CaCl_2$ would not have led to the identification of the TICC1 in our case but to a mixture of the binary ICC1 and ICC2. Based on Scheme 1 and some further grinding experiments, a full ternary solid-state phase diagram of the LEV–INA–$CaCl_2$ system was built, as shown in Fig. 4. Using this diagram, the thermodynamic outcome of any solid-state grinding experiment can be predicted, as it shows the most stable outcome for a given combination of reactants. Similar diagrams are obtained for the ETI–INA–$CaCl_2$ and LEV–NA–$CaCl_2$ system (see the section of solid-state behavior for TICCs in the ESI†).

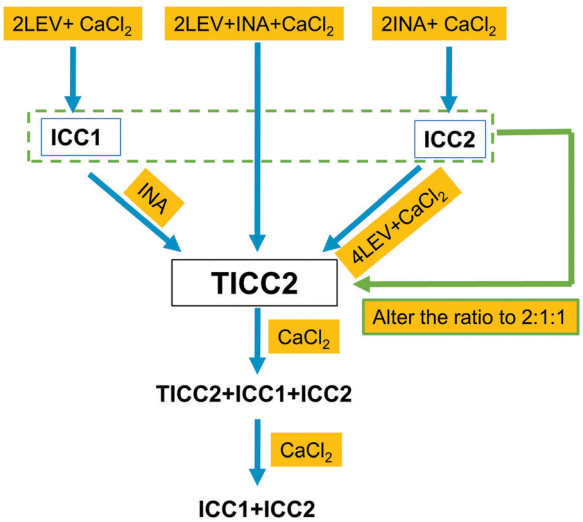

Scheme 1 Graphic representation of the LEV–INA–$CaCl_2$ solid-state reaction scheme according to overall stoichiometry.

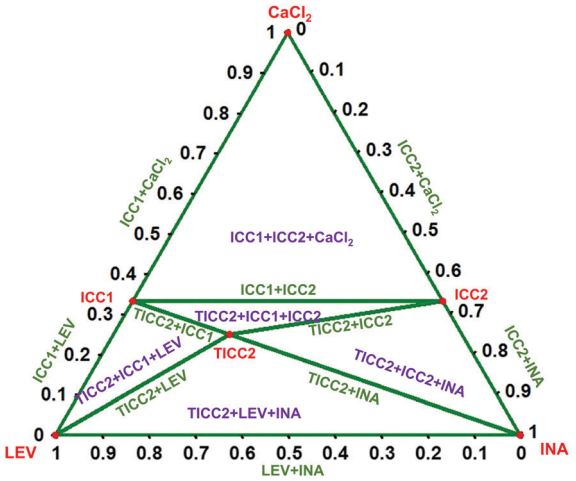

Fig. 4 Solid-state ternary phase diagram for the LEV–INA–$CaCl_2$ system. Pure phases are indicated in red, mixtures of two phases in green and mixtures of three phases in purple. Sufficient H_2O is considered for the formation of all ICCs.

Interestingly, for this latter system, full transformation to TICC3 was difficult to achieve during the grinding experiments, with the binary ICCs usually being formed prior to the TICC. It is possible that in this case, the presence of the binary ICCs hinders the nucleation of the TICC during grinding.

All TICCs discussed above are monohydrates. These monohydrates are formed in all experiments throughout this work, even those performed in hydrophobic solvents. Ambient water seemingly needs to be present in extremely low activity for the monohydrates to form. The key role of this water molecule for the stability of the TICCs becomes clear, when investigating their thermal behavior. Heating the TICCs, a weight loss of about 3% occurs between 100 °C and 150 °C corresponding to the loss of 1 equivalent of water (theoretical weight loss = 3.1%) (TGAs given in ESI†). This initial weight loss is immediately followed by a weight loss of about 20%, in the case of TICC1 and TICC2, corresponding to the loss of the INA equivalent, which continues up to 200 °C. For TICC3 (Fig. S21, ESI†), both phenomena are well separated, with no weight loss occurring between 110 and 150 °C. To investigate the potential existence of an anhydrate TICC, TICC3 was kept at 100 °C for a prolonged period and regularly analyzed by XRPD (Fig. S24, ESI†). This evaluation shows a decrease of TICC3 with surprisingly a simultaneous appearance of a mixture of NA and the binary anhydrous cocrystal $LEV_2{\cdot}CaCl_2$. Furthermore, cooling this mixture to room temperature in an ambient atmosphere leads to a mixture of NA and the hydrated binary cocrystal ICC1 (Fig. S25, ESI†). Heating the TICCs to a temperature of 200 °C (above the removal of NA and INA), and cooling them under ambient conditions always led to the binary hydrated cocrystals involving LEV/ETI.

These results highlight the crucial role of water for the formation of these TICCs, as they are thermodynamically unstable without presence of this water equivalent, decomposing subsequently in an anhydrous binary ICC and one of the composing partners. From our screening experiments, it is however evident, that traces of water suffice to allow their formation.

To explore the potential of dual-drug TICCs, we investigated their impact on the solubility of both drug compounds, comparing the values of isolated drugs with that of binary and ternary ionic cocrystals. To get a fair comparison, we first aimed at identifying a solvent in which binary, as well as ternary ionic cocrystals behave congruently. Table S4 (ESI†) shows the suspension outcome performed under the stoichiometry of binary as well as ternary cocrystals using 12 different solvents. The binary systems ICC1 and ICC2 were almost always found to behave incongruently (except for ICC1 in an acidic water environment), whereas ICC3 behaves congruently in water, ethanol, isopropanol, and ethyl acetate. Surprisingly, the ternary systems, are more inclined to behave congruently, especially in the case of TICC2, which behaves congruently in water, as well as a variety of polar solvents like methanol, ethanol and acetone. This implies that from a pharmaceutical point of view, dual drug ternary cocrystals, can have an advantage over a combination of their binary counterparts.

We determined the solubilities of parent drugs, binary and ternary ionic cocrystals for all congruent systems (Table S5, ESI†). In a pH 1.2 HCl aqueous solution the solubility of NA increases from 44.20 to 49.95 wt% comparing to the parent compound with the binary ICC. The TICCs on the other hand seem to show a reduced solubility compared to both parent drug compounds. Binary ICCs and ternary ICCs therefore impact drug solubility differently, and it will be interesting in the future to compare bioavailability of TICCs to see if the differences in solubility also reflect in the pharmacokinetics.

In this work, we proposed a new strategy to design multi-drug solid forms. Using an inorganic salt as the glue sticking two different APIs together in a ''drug-bridge-drug'' approach, we successfully created three different ternary ionic cocrystal (TICCs). Furthermore, our approach involves pharmaceutically acceptable salts such as $CaCl_2$, leading to pharmaceutically suitable solid forms. We furthermore highlighted the importance of the overall stoichiometry for the stability of these ternary systems, investigating the full solid-state ternary phase diagram. Water plays a crucial role for the stability of these systems, with trace amounts sufficient to lead to their formation. Finally, these systems impact the solubility of both drug compounds, and it will therefore be interesting in the future to see how these ternary systems behave with respect to the parent drug compounds in *in vivo* studies. We expect the strategy presented here, to be applicable to a large series of drug combinations, opening up a promising new way of building multi-drug systems.

Lixing Song would like to thank the China Scholarship Council (CSC) for financial support. The authors would like to thank the FNRS for funding (grants T.0149.19 and T.0262.20).

Conflicts of interest

There are no conflicts to declare.

Notes and references

‡ No water was added in the grinding experiments, but the hygroscopicity of $CaCl_2$ and the ambient relative humidity always led to hydrate formation.

1 A. I. Wertheimer and A. Morrison, *P&T*, 2002, **27**, 44–49.
2 F. Simon, *Nat. Rev. Drug Discovery*, 2006, **5**, 881–882.
3 B. S. Sekhon, *Daru, J. Pharm. Sci.*, 2012, **20**, 45.
4 R. Thipparaboina, D. Kumar, R. B. Chavan and N. R. Shastri, *Drug Discovery Today*, 2016, **21**, 481–490.
5 L. Feng, P. H. Karpinski, P. Sutton, Y. Liu, D. F. Hook, B. Hu, T. J. Blacklock, P. E. Fanwick, M. Prashad, S. Godtfredsen and C. Ziltener, *Tetrahedron Lett.*, 2012, **53**, 275–276.
6 F. Liu, Y. Song, Y.-N. Liu, Y.-T. Li, Z.-Y. Wu and C.-W. Yan, *Cryst. Growth Des.*, 2018, **18**, 1283–1286.
7 R. Santra, N. Ghosh and K. Biradha, *New J. Chem.*, 2008, **32**, 1673–1676.
8 D. Braga, F. Grepioni, L. Maini, S. Prosperi, R. Gobetto and M. R. Chierotti, *Chem. Commun.*, 2010, **46**, 7715–7717.
9 T. T. Ong, P. Kavuru, T. Nguyen, R. Cantwell, L. Wojtas and M. J. Zaworotko, *J. Am. Chem. Soc.*, 2011, **133**, 9224–9227.
10 H. Oertling, *CrystEngComm*, 2016, **18**, 1676–1692.
11 D. P. Karothu, I. Jahović, G. Jovanovski, B. Kaitner and P. Naumov, *CrystEngComm*, 2017, **19**, 4338–4344.
12 D. Braga, F. Grepioni and O. Shemchuk, *CrystEngComm*, 2018, **20**, 2212–2220.
13 K. Linberg, N. Z. Ali, M. Etter, A. A. L. Michalchuk, K. Rademann and F. Emmerling, *Cryst. Growth Des.*, 2019, **19**, 4293–4299.
14 S. Bhattacharya, K. S. Peraka and M. J. Zaworotko, *Co-crystals: Preparation, Characterization and Applications*, The Royal Society of Chemistry, 2018, pp. 33–79.
15 D. Braga, F. Grepioni, G. I. Lampronti, L. Maini and A. Turrina, *Cryst. Growth Des.*, 2011, **11**, 5621–5627.
16 D. Braga, F. Grepioni, L. Maini, D. Capucci, S. Nanna, J. Wouters, L. Aerts and L. Quere, *Chem. Commun.*, 2012, **48**, 8219–8221.
17 A. J. Smith, S. H. Kim, N. K. Duggirala, J. Jin, L. Wojtas, J. Ehrhart, B. Giunta, J. Tan, M. J. Zaworotko and R. D. Shytle, *Mol. Pharmaceutics*, 2013, **10**, 4728–4738.
18 J. Wouters, F. Grepioni, D. Braga, R. M. Kaminski, S. Rome, L. Aerts and L. Quéré, *CrystEngComm*, 2013, **15**, 8898–8902.
19 A. R. Buist and A. R. Kennedy, *Cryst. Growth Des.*, 2014, **14**, 6508–6513.
20 N. K. Duggirala, A. J. Smith, Ł. Wojtas, R. D. Shytle and M. J. Zaworotko, *Cryst. Growth Des.*, 2014, **14**, 6135–6142.
21 F. Grepioni, J. Wouters, D. Braga, S. Nanna, B. Fours, G. Coquerel, G. Longfils, S. Rome, L. Aerts and L. Quere, *CrystEngComm*, 2014, **16**, 5887–5896.
22 N. K. Duggirala, M. L. Perry, O. Almarsson and M. J. Zaworotko, *Chem. Commun.*, 2016, **52**, 640–655.
23 L. Mazzei, V. Broll, L. Casali, M. Silva, D. Braga, F. Grepioni, J. Baltrusaitis and S. Ciurli, *ACS Sustainable Chem. Eng.*, 2019, **7**, 13369–13378.
24 A. Hovinga Collin, *Pharmacotherapy*, 2001, **21**, 1375–1388.
25 A. H. Gouliaev and A. Senning, *Brain Res. Rev.*, 1994, **19**, 180–222.
26 M. Knip, I. F. Douek, W. P. T. Moore, H. A. Gillmor, A. E. M. McLean, P. J. Bingley, E. A. M. Gale and European Nicotinamide Diabetes Intervention Trial Group, *Diabetologia*, 2000, **43**, 1337–1345.
27 M. Sowa, K. Slepokura and E. Matczak-Jon, *Acta Crystallogr.*, 2013, **69**, 1267–1272.
28 L. S. Reddy, N. J. Babu and A. Nangia, *Chem. Commun.*, 2006, 1369–1371.
29 S.-W. Zhang, A. P. J. Brunskill, E. Schwartz and S. Sun, *Cryst. Growth Des.*, 2017, **17**, 2836–2843.
30 H. E. Kerr, L. K. Softley, K. Suresh, A. Nangia, P. Hodgkinson and I. R. Evans, *CrystEngComm*, 2015, **17**, 6707–6715.
31 L. Song, O. Shemchuk, K. Robeyns, D. Braga, F. Grepioni and T. Leyssens, *Cryst. Growth Des.*, 2019, **19**, 2446–2454.
32 J. Xue, Y. Jiang, W. Li, L. Yang, Y. Xu, G. Zhao, G. Zhang, X. Bu, K. Liu, J. Chen and J. Wu, *Spectrochim. Acta, Part A*, 2015, **137**, 864–870.
33 D. Braga, F. Grepioni, G. I. Lampronti, L. Maini, K. Rubini, A. Turrina and F. Zorzi, *CrystEngComm*, 2014, **16**, 7452–7458.
34 G. Springuel, K. Robeyns, B. Norberg, J. Wouters and T. Leyssens, *Cryst. Growth Des.*, 2014, **14**, 3996–4004.

